Biosensors and Bioelectronics 164 (2020) 112338

Contents lists available at ScienceDirect

Biosensors and Bioelectronics

journal homepage: http://www.elsevier.com/locate/bios

Real-time glucose monitoring system containing enzymatic sensor and enzymatic reference electrodes

Lukas Ramašauskas [a], Rolandas Meškys [b], Dalius Ratautas [a,b,*]

[a] Faculty of Fundamental Sciences, Vilnius Gediminas Technical University, Saulėtekio al. 11, LT-10223, Vilnius, Lithuania
[b] Institute of Biochemistry, Life Sciences Center, Vilnius University, Saulėtekio al. 7, LT-10257, Vilnius, Lithuania

ARTICLE INFO

Keywords:
Glucose
Biosensor
Laccase
Glucose dehydrogenase
Enzymatic reference electrode
Self-reference

ABSTRACT

Every electrochemical biosensor uses two or three electrode setup, which involves sensing electrode for a specific reaction, metal/salt reference electrode (i.e., Ag/AgCl or Hg/Hg_2Cl_2) for the control of the potential and, is some cases, counter electrode for the compensation of the current. This setup has significant flaws related to metal/salt reference electrodes: they are bulky and difficult to miniaturize, leak electrolyte to the medium, lose the ability to define the electrochemical potential precisely in time, consequently, have to be updated or replaced. This causes problems when the biosensor cannot be easily replaced (e.g., implanted electronics). Here we present a fully enzymatic real-time glucose monitoring system capable of referencing its own electrochemical potential. Using sensing electrode composed of wired glucose dehydrogenase and enzymatic reference electrode composed of wired laccase we have created a stable and accurate electrode system, which measured fluxes in concentration of glucose in a physiological range (3–8 mM), and demonstrated performance of the designed system in undiluted human serum. In addition, our designed enzymatic reference electrode is universal and may be applied for other biosensors, thus open possibilities for the new generation of implantable devices for healthcare monitoring.

1. Introduction

Electrochemical biosensors were proposed in 1962, then Clark and Lyons presented the idea of electrodes for glucose sensing (Clark and Lyons, 1962). Since then, nearly every biosensor is composed of two or three electrodes: a sensing electrode with specific enzyme responsible for a recognition reaction, a metal/salt reference electrode, which controls the potential (Ag/AgCl or Hg/Hg_2Cl_2), and, in some cases, a counter electrode for the compensation of electric current (Windmiller and Wang, 2013). In the past decades, significant attention has been given to the development and improvements of a key element of biosensors – sensing electrodes. Those electrodes have been designed by wiring the specific enzymes using different strategies. Hence, three generations of biosensors differing one from another by the mechanism of electron transfer between an enzyme and electrode surface have been developed (Wang, 2008). Many of the 1^{rst} the and 2nd generation biosensors have been designed for an indirect (mediated) electron transfer (Ramonas et al., 2019; Scheller et al., 1991). Recently attention has been given to a direct electron transfer between the enzyme and electrode for the construction of the 3rd generation biosensors, which are mediator- and label-free, avoid interference and possess superior sensitivity (Das et al., 2016; Stoica et al., 2006; Gineitytė et al., 2019; Ratautas et al., 2017). Some of the 3rd generation electrodes have been designed for continuous glucose monitoring, e.g., an electrode, which could measure glucose concentration up to 9 days has been produced (Lee et al., 2019) or wireless biosensing (Larpant et al., 2019). The emergence of implantable electronics for health monitoring or power production *in vivo* requires a new alternative for the control of potential, since typical metal/salt electrodes are poorly suited for operation *in vivo*: i) they are difficult to miniaturize, ii) leak electrolyte to the surrounding media and iii) may cause severe immune response and, as a result, iv) lose the ability to control potential, thus need to be renewed or replaced (Hashemi et al., 2011). We note that significant potential drifts for *in vivo* tested metal/salt reference electrodes (Ag/AgCl or Hg/Hg_2Cl_2) were noticed as early as in 1986 (Thompson and Vandenberg, 1986), yet little efforts were reported to solve the above-mentioned issues, despite significant advances in the development of sensor electrodes. The majority of the reported studies have been focusing on improvement and miniaturization of the current technology – metal/salt reference electrodes (Shinwari et al., 2010).

In this work we present a new approach in designing biosensors, which could be implemented for future implantable electronics as

* Corresponding author. Institute of Biochemistry, Life Sciences Center, Vilnius University, Saulėtekio al. 7, LT-10257, Vilnius, Lithuania.
E-mail address: Dalius.Ratautas@gmc.vu.lt (D. Ratautas).

https://doi.org/10.1016/j.bios.2020.112338
Received 5 March 2020; Received in revised form 15 May 2020; Accepted 28 May 2020
Available online 30 May 2020

healthcare monitoring devices. We have designed a real-time glucose biosensing system composed of two electrodes: a sensor electrode with immobilized glucose dehydrogenase and an enzymatic reference electrode with immobilized laccase (Fig. 1). A sensing electrode catalyzed the oxidation of glucose – its electrochemical potential was depended on glucose concentration. An enzymatic reference electrode catalyzed oxygen reduction reaction (ORR) – its potential was very stable during multiple measurements. Additionally, we have tested a performance of the biosensor system in buffer solutions mimicking human blood, designed protection membrane to remove the effects of interfering substances (e.g. ascorbic acid, urea, ethanol and acetaminophen), demonstrated the capability of biosensing system to measure glucose concentrations in physiological concentration range of 3–8 mM in real-time, as well as tested the performance of biosensor using real human serum.

2. Experimental section

2.1. Materials

Gold (III) chloride trihydrate, sodium citrate, 5% Nafion® 117 solution, 4-mercaptobenzoic acid (4-MBA), ethanol, methanol, acetaminophen, L-ascorbic acid, multi-walled carbon nanotubes (MWCNT), $NaH_2PO_4{\cdot}2H_2O$, Na_2CO_3, KCl, NaCl, $CaCl_2$, $MgCl_2$, $CO(NH_2)_2$, H_2SO_4, KOH, $HClO_4$, NaOH, glucose were purchased from Sigma-Aldrich. Glucose dehydrogenase (GDH) from *Ewingella americana* was produced and purified as described (Ratautas et al., 2015). In addition to glucose, enzyme can also oxidize lactose, however, with lower rate – k_{cat}/K_M ratio for glucose and lactose was 665 M^{-1} s^{-1} and 196 M^{-1} s^{-1}, respectively (Ratautas et al., 2018). The concentration of GDH stock solution was 24 mg mL^{-1}. Laccase from *Didymocrea* sp. (LAC) was purified as described (Tetianec et al., 2014). The concentration of LAC stock solution was 15.8 mg mL^{-1}. Human serum sample was purchased from Sigma-Aldrich. The serum sample was received from male of USA origin was sterile and filtered by the supplier. The concentration of glucose in a sample was 4.2 mM and pH – 8.12. The serum sample was used for measurements without any additional modifications. All experiments were carried using working buffer solution (WBS), where the concentrations of key electrolytes were similar to those in human blood serum (Häggström, 2014): 25 mM NaH_2PO_4 ·$2H_2O$, 25.5 mM Na_2CO_3, 4.4 mM KCl, 90 mM NaCl, 2.4 mM $CaCl_2$, 0.84 mM $MgCl_2$, 5.2 mM CO $(NH_2)_2$, pH was adjusted to 7.4 using HCl.

Gold nanoparticles (AuNPs) and MWCNT solutions were prepared using procedures described below. AuNPs were synthesized using $HAuCl_4{\cdot}3H_2O$ and trisodium citrate according to the revised Turkevich synthesis method (Kimling et al., 2006). Afterwards, the AuNPs were concentrated by the means of centrifugation (13000 rpm, 15 min). Around 90% of supernatant was removed, the remaining dispersion was collected in a new test-tube and the procedure was repeated one more time. The diameter of AuNPs and concentration of prepared stock solution were determined to be 10 nm and 1.42 μM using spectrophotometric method (Haiss et al., 2007) and confirmed using atomic force microscopy measurements (AFM) (Supplementary Information (SI), Fig. S1). The solution of MWCNT was prepared by placing 5.0 mg of MWCNT into 1.0 mL of deionized water and keeping in a ultrasound bath for 24 h. The diameter of MWCNT was determined to be 7 ± 5 nm according to the AFM analysis (SI, Fig. S1).

2.2. Electrode preparation procedures

Sensor electrode (Sensor) preparation. Firstly, gold electrodes were polished by using fine-grit pad surface, obtained from BASi, wetted with deionized water, later sonicated in deionized water for 10 min. Afterwards, the electrodes were rinsed thoroughly with deionized water and treated using following electrochemical cleaning procedure. Briefly, 40 CV scans were run from 0 to –2600 mV and backwards in 0.05 M KOH solution, followed by 40 cycles from –200 to 1750 mV and backwards in 0.5 M H_2SO_4. In both cases potential scan rate was 300 mV s^{-1}. Afterwards, electrodes were thoroughly rinsed with deionized water. Next, the AuNPs deposition was performed on the surface of the gold electrodes by placing 2 μL of AuNPs and allowing to dry at room temperature. Once the surface has been dried, the electrodes were rinsed with

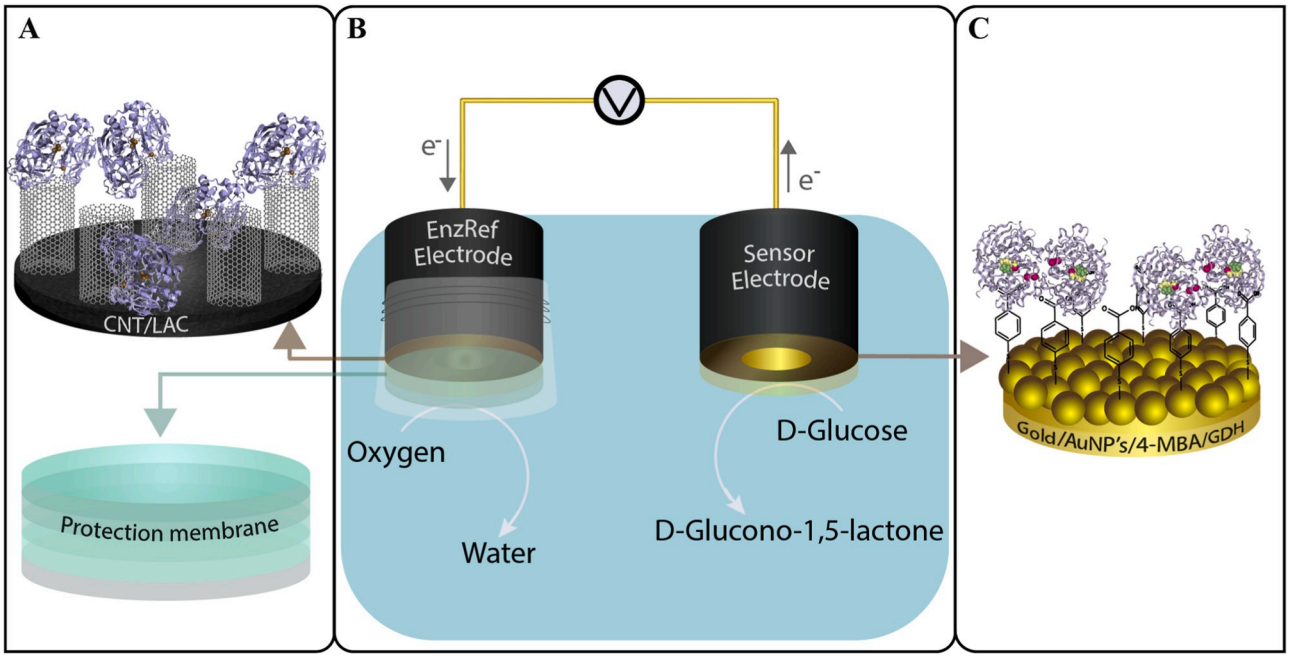

Fig. 1. A) Enzymatic reference electrode composed of carbon electrode with immobilized carbon nanotubes and laccase (EnzRef). To ensure stable electrochemical potential, the electrode was additionally covered by protective membrane. **B)** The designed real-time glucose monitoring system (GluSens) with enzymatic sensor and reference electrodes. **C)** Enzymatic sensor electrode (Sensor) composed of gold electrode modified with gold nanoparticles, 4-mercaptobenzoic acid and glucose dehydrogenase. (For interpretation of the references to colour in this figure legend, the reader is referred to the Web version of this article.)

deionized water and submerged in a 5 mM 4-MBA solution in methanol and left in a sealed test-tube for overnight. Finally, the electrodes were thoroughly rinsed with methanol and then with deionized water and 2 μL of GDH stock solution was placed on top and left for 2 h at room temperature under humid conditions to avoid the evaporation of the enzyme solution (SI, Fig. S2).

Enzymatic reference electrode (EnzRef) preparation. Firstly, a cylindrical surface of graphite rod electrode was isolated using heat-shrinking tube and a planar side was polished using emery paper (200 μm). Then, the electrodes were thoroughly rinsed with deionized water and dried using pure argon. Next, 5 μl solution containing 5 mg ml^{-1} MWCNT in water was placed on the surface and left to dry at room temperature. Afterwards, 2 μl of LAC solution was placed on the electrode and left to dry at room temperature. Finally, the electrodes were modified by placing 10 μl solution containing 2% neutralized Nafion® in ethanol on the surface and allowed to dry at 4 °C. Protective membrane was made from cellulose filter paper and multiple Nafion® layers. First, the filter paper was cut the size and shape of electrode surface. Then, 7 μl of 5% Nafion® solution was placed on the cellulose filter paper and left to dry at 4 °C. The deposition of the polymer was repeated 5 times, as a result, 5 layers of Nafion® polymer were formed. Finally, a prepared membrane was carefully placed on the surface of the laccase electrode and covered by 500 Da cut-off dialysis membrane (SI, Fig. S2).

2.3. Methods

Electrochemical experiments were performed with Gamry Reference 600^{TM} potentiostat. Chronoamperometric and cyclic voltammetry measurements were carried out in a three-electrode glass cell using a saturated calomel electrode (SCE, 244 mV *vs.* SHE) as a reference electrode. Platinum foil electrode (surface area 1.65 cm^2) was used as a counter electrode, gold electrode (0.02 cm^2) was used for constructing Sensor and graphite electrode (0.071 cm^2) for EnzRef electrodes. Chronopotentiometric measurements (when Sensor and EnzRef electrodes were analyzed electrochemically) were carried out in a two-electrode glass cell using only electrode of interest (Sensor or EnzRef) and a SCE for the reference of electrochemical potential. Real-time glucose measurements and analysis of the designed glucose monitoring system containing Sensor and EnzRef electrodes (GluSens) were conducted using chronopotentiometry. EnzRef electrode was used as a potential reference (450 mV *vs*. SCE (694 mV *vs*. SHE)). All the electrochemical measurements were performed in a 20 ml electrochemical cell containing 10 mL WBS.

Surface morphology analysis of the synthesized electrodes and the size of AuNPs and MWCNT were analyzed using Dimension Icon AFM from Bruker. The microscope was used in ScanAsyst Air mode using ScanAsyst-Air probes. The surface morphology of prepared electrodes, but without protective (or dialysis) membranes, was registered using electrodes as described above. The analysis of AuNPs (or MWCNT) was conducted by placing 10 μL of AuNPs (or MWCNT) solution on the freshly prepared mica plate and allowing to dry for 2 h.

3. Results and discussion

3.1. Analysis of enzymatic sensor (Sensor) electrode

To design the Sensor electrode, we have used glucose dehydrogenase from *Ewingella americana* (GDH). We have demonstrated in our previous works that this enzyme is capable of direct electron transfer (DET) with many nanomaterials, thus it gave us possibility to create the 3rd generation sensor (Ratautas et al., 2015, 2018). GDH was immobilized on 4-mercaptobenzoic acid (4-MBA) and gold nanoparticles (AuNPs) modified gold electrode (Fig. 1C). Though GDH could achieve a more effective DET on different surface modifications, the rationale to use 4-MBA was to achieve a more stable system – 4-MBA-gold monolayers had a higher surface coverage and stability compared to other thiols (Barriet et al., 2007). The rationale to use AuNPs instead of planar gold was based on several factors: AuNPs increase the surface are of the electrode (Pingarrón et al., 2008), may actively participate in electron transfer reactions via electron mediation (Kizling et al., 2018), and, for some enzymes, may facilitate a direct electron transfer between the protein and the electrode surface (Ratautas and Dagys, 2019). At first, the designed Sensor electrode was analyzed using cyclic voltammetry (CV) from –300 to 300 mV *vs.* SCE (Fig. 2A). When no glucose was present, no biocatalytic process was observed in an analyzed potential range. After 10 mM glucose was added, a biocatalytic current started from around –200 mV, indicating Sensor electrode activity towards glucose. For glucose concentration measurements, we have chosen to observe the change in the open circuit potential (OCP) of the electrode after the addition of glucose. OCP depends on the ratio of oxidized and reduced enzyme forms and should change when glucose is present according to the Nernst equation. Chronoamperometric measurements showed OCP was around –90 mV without glucose. When 1 mM glucose was added the potential dropped to –195 mV (Fig. 2B). Repeated additions of glucose (1 mM) resulted in a decrease in OCP of the electrode. To demonstrate that potential decrease was not a random, but well predictable physical process, the OCP dependence on glucose concentration was plotted and fitted to Nernst equation (Fig. 2C). The fit revealed an excellent correlation between experimental data and the model and demonstrated that OCP measurements could be used to determine the concentration of glucose in range 1–8 mM. We have noticed that initial OCP values of the electrodes without glucose could not be easily reproduced and varies from –50 to –100 mV for different batches. Most likely, this difference resulted from slightly diverse conditions when preparing electrodes. However, the difference between potential values of different concentration of glucose was very precise for each

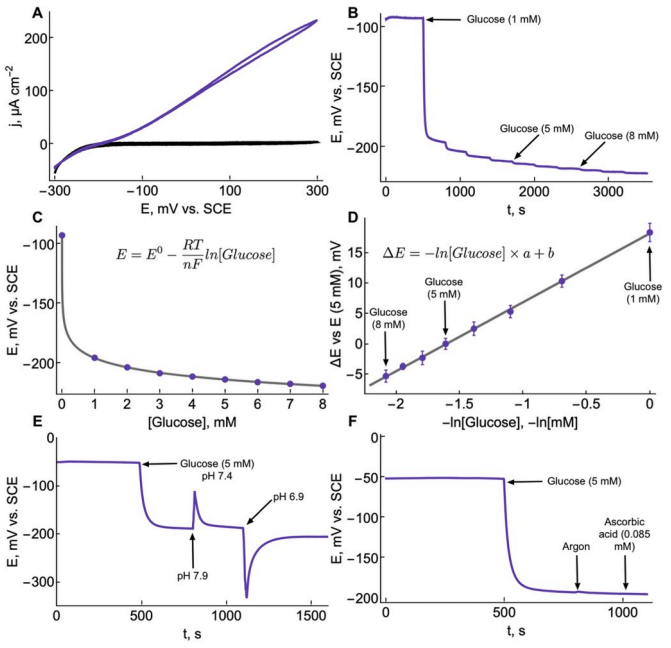

Fig. 2. The electrochemical analysis of Sensor electrode. **A**) CVs demonstrating current density dependence on applied potential without glucose (black) and with 10 mM glucose (purple). Potential scan rate – 10 mV s^{-1}. **B**) Potential dependence on increase in glucose concentration. **C**) Potential dependence on increase in glucose concentration fitted to Nernst equation. **D**) A linearized potentiometric calibration curve depending on glucose concentration (0–8 mM). **E**) Potential dependence on pH change in the measurement medium. **F**) Potential dependence on glucose concentration and interference (argon bubbling, ascorbic acid). Blood mimicking WBS pH 7.4. Potential was measured in reference to SCE (0.244 V *vs.* SHE). (For interpretation of the references to colour in this figure legend, the reader is referred to the Web version of this article.)

measurement (<0.2 mV).

For those reasons, we have decided to calibrate the Sensor electrode by measuring the difference between the electrode OCP value at any given concentration of glucose, with OCP value at 5 mM glucose concentration. This method resulted in reproducible calibration curves – the OCP difference at 5 mM glucose was set to zero (Fig. 2D). Finally, we have evaluated performance of the electrode in case of pH shifts and in the presence of additional interference – decrease in oxygen concentration (argon bubbling) and ascorbic acid. In Fig. 2E potential was measured at pH 7.4. After the addition of 5 mM glucose, pH was changed to 7.9 and after a few minutes to 6.9. The electrode potential did not completely recover to the initial value, thus data indicates that Sensor electrode should be used with care, if the changes in pH are expected. Additionally, neither argon bubbling (oxygen removal), nor addition of ascorbic acid (0.085 mM) resulted in any observable change in electrode potential (<0.2 mV) (Fig. 2F).

In addition, we have evaluated the surface morphology of the designed electrode using AFM (SI, Fig. S3). The analysis demonstrated the tightly packed layers of AuNPs forming "nanomountains" with difference between peaks and craters of 1–2 μm. The analysis of images showed that distinct AuNPs were not visible well even using a high magnification (in comparison to bulk AuNPs in SI, Fig. S1). Mostly likely, the addition of surface modifications as well as enzymes formed a "soft" surface and curvatures of solitary AuNPs were not visible. In addition, the AFM images showed that modification using AuNPs greatly increased a surface area of the electrode.

3.2. Analysis of enzymatic reference (EnzRef) electrode

To create enzymatic electrode, which could replace metal/salt reference electrodes as a reference for potential, we had to select the most suited enzyme-catalyzed electrochemical reaction. We have chosen ORR:

$$O_2 + 4H^+ + 4e^- \rightarrow 2H_2O \quad (1)$$

The potential of ORR depends on pH and oxygen concentration, which are very stable in a context of application for implantable electronics. In human body both pH and oxygen concentration differ in specific organs, but are very stable in the same tissue, e.g., oxygen concentration in skin epidermis is kept around 0.01 mM (Shleev, 2017), while pH of blood and interstitial fluid normally is kept 7.35–7.45 (Proksch, 2018). Additionally, ORR is catalyzed by a group of enzymes – multicopper oxidases and some of them are capable of the DET (Shleev et al., 2005; Falk et al., 2012). For those reasons, laccase from *Didymocrea* sp. was used to create EnzRef electrode. We have used this enzyme previously to design high performance electrodes as well as demonstrated that this enzyme is very resistant to inhibition resulting from Cl^- and F^- ions (Dagys et al., 2017; Ratautas et al., 2018). At first, the enzyme was immobilized on the carbon-based electrode surface prior modified by carbon nanotubes (CNT) and electrochemical analysis of electrode performance was conducted. The rationale to use CNT was based on our previous experience demonstrating a fast electron transfer between laccase and CNT (Ratautas et al., 2015) as well as other research paper indicating that CNT and their composites can improve electron transfer capabilities of laccases (Gutiérrez-Sánchez et al., 2012). CVs demonstrated a biocatalytic ORR catalyzed by the electrode in an air saturated buffer solution beginning from 430 mV *vs.* SCE (Fig. 3A). When oxygen was removed from the solution by argon bubbling, a significant decrease in ORR current was observed. Additionally, we have measured an amperometric ORR current at 200 mV *vs.* SCE (Fig. 3B). It was demonstrated that the electrode was indeed active and reduced oxygen to water – the removal of oxygen resulted in an apparent decrease in current. We have also evaluated the electrode performance as an enzymatic reference electrode. OCP was measured adding interfering compounds (glucose and ascorbic acid) and after changing pH of the media (Fig. 3CD). Though OCP was stable after the addition of glucose and the change in pH did not result in any unexpected potential shifts, the electrode was very affected after the addition of ascorbic acid. Such drop in OCP demonstrate that electrode design must be improved to eliminate the interference of ascorbic acid, otherwise potential readings cannot be used as reference. For this reason, we have designed a specific protective membrane, which was placed directly on the electrode surface (Fig. 1A). The usage of a protective membrane significantly decreased the ORR rate catalyzed by the electrode, yet the electrode remained active (Fig. 3A'B'). Finally, we have tested the effect on OCP of the electrode using glucose, ascorbic acid and by changing pH of reaction medium (Fig. 3C'D'). After a few minutes electrode potential stabilized to 450 mV *vs.* SCE and neither glucose nor ascorbic acid resulted in any noticeable effect on OCP value (<0.2 mV). The change in pH from 7.4 to 6.9 and to 7.9 did not result in electrode destabilization and activity drop either.

In addition, we have evaluated the surface morphology of the designed electrode, thus we have carried AFM measurements of EnzRef electrode without using protective or dialysis membranes (SI, Fig. S4). The analysis demonstrated a "weblike" structures with peaks and craters of 1–1.5 μm. Images using the higher magnification demonstrated that

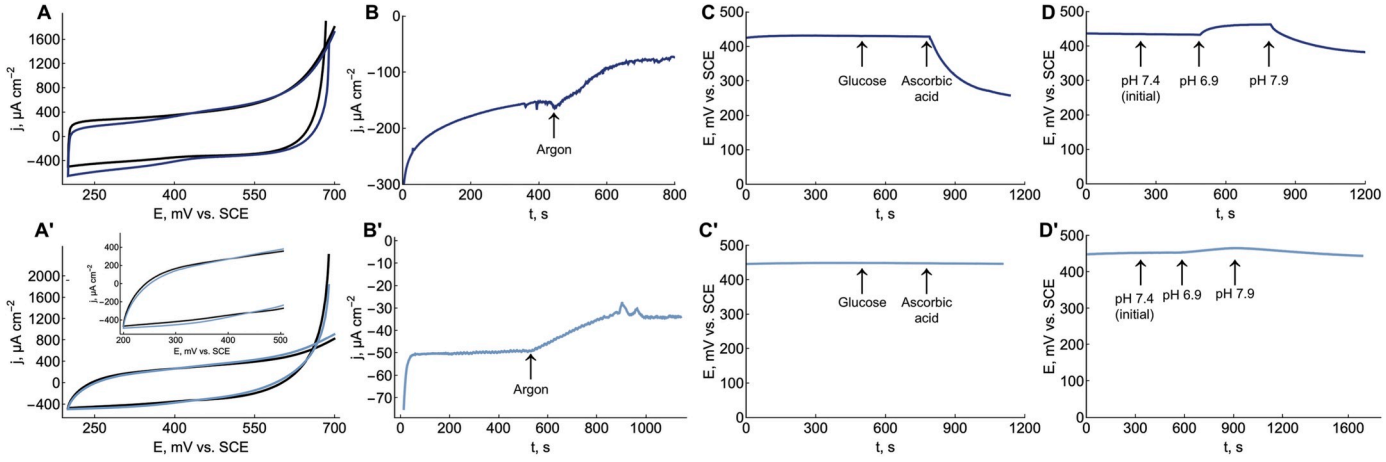

Fig. 3. The electrochemical analysis of enzymatic reference electrode without protective membrane (**A**–**D**) and with protective membrane (**A′**-**D′**). **A**, **A′**) CVs demonstrating current density dependence on applied potential in air (blue) and argon (black) saturated buffer solutions. Potential scan rate – 10 mV s^{-1}. **B**, **B′**) Chronoamperometric curves at fixed potential (at 200 mV) in air saturated buffer solution and under argon bubbling. **C**, **C′**) OCP dependence on interfering substances (glucose and ascorbic acid). **D**, **D′**) OCP dependence on pH changes in the measurement medium. Blood mimicking WBS pH 7.4. Potential was measured in reference to SCE (0.244 V *vs.* SHE). (For interpretation of the references to colour in this figure legend, the reader is referred to the Web version of this article.)

MWCNT were packed together randomly with significant gaps between nanotubes. In addition, comparing images of bulk nanotubes (SI, Fig. S1) and nanotubes with the immobilized enzyme (SI, Fig. S4) it could be seen that the surface became softer, and the nanotubes were covered with the spherical particles of the diameter of 4 ± 1 nm, most likely consisting of enzyme molecules or enzyme aggregates. In addition, images demonstrated that the surface area of the electrode was greatly increased by the immobilized MWCNT.

3.3. Designing real-time glucose monitoring system (GluSens) by combining Sensor and EnzRef electrodes

To demonstrate that EnzRef electrode could replace typical metal/salt electrodes for biosensing applications we have created glucose biosensing system, which contained both electrodes: Sensor and EnzRef (Fig. 1B). We have named this electrode system GluSens. Sensor electrode catalyzed the oxidation of glucose, while EnzRef – ORR. Total bioelectrochemical process was:

$$2Glucose + \ O_2 \rightarrow Gluconolactone + 2H_2O \quad (2)$$

The potential of reaction (2) depends on concentrations of glucose and oxygen. We have demonstrated that EnzRef electrode had a stable OCP, which was not significantly influenced by the changes in oxygen concentration. It is expected that a potential difference between Sensor and EnzRef electrodes would correlate with the concentration of glucose. At first, we have tested the performance of the GluSens electrode system in the presence of interference (Fig. 4A and SI, Fig. S5). After the addition of 5 mM glucose, the OCP was –650 mV *vs.* EnzRef. The addition of ascorbic acid (0.085 mM) did not result in any change in OCP (<0.2 mV). When argon gas was bubbled through solution the OCP value increased to –648 mV. We have tested additional interfering substances – urea, ethanol and acetaminophen (paracetamol) (SI, Fig. S5). No significant interference was observed and only ascorbic acid started to cause small interference at concentrations higher than 0.1 mM (SI, Fig. S5). Then we tested GluSens system operation dependence on pH shifts (Fig. 4B). After the addition of 5 mM glucose at pH 7.4, the OCP value was –650 mV *vs.* EnzRef. A sudden change in pH from 7.4 to 6.9 resulted in a positive spike in OCP value to –561 mV *vs.* EnzRef, which later dropped below an initial OPC value. Afterwards, pH of medium was changed to 7.9 and it caused another, yet negative, spike in OCP value reaching –864 mV *vs.* EnzRef, which later increased above the initial OCP value. Data demonstrated that GluSens electrode system was sensitive and could be interfered by the radical changes in pH value (±0.5). Afterwards, electrode system was calibrated by measuring OCP values depending on concentration of glucose (Fig. 4C). Decrease in OCP value was related to the concentration of glucose (at 5 mM glucose OCP was –645 mV *vs.* EnzRef). Data was fitted to Nernst equation demonstrating a good agreement between experimental results and the model. Since, we have observed a difference in OCP values between different batches of electrodes (e.g. OCP at 5 mM glucose could differ around ±10 mV for different electrode batches), we have used a calibration curve where the native logarithm of glucose concentration was plotted against the difference in potential between the measured OCP value and the OCP value at 5 mM glucose (Fig. 4D). In this way, we have received highly reproducible calibration curves between different batches of electrodes composing GluSens system. According to our method, the OCP value at 5 mM glucose was set to zero for each measurement. We have also evaluated a reproducibility, a storage stability and a limit of detection of the GluSens electrode system. Six calibration curves from different batches of electrodes were created, and reproducibility was calculated ±11.2% from the average value of the slopes, demonstrating a good repeatability (data not shown). In addition, we have evaluated a storage stability of the GluSens system. A calibration curve using the developed electrode system was recorded for 10 days and the normalized values of slopes were plotted against time (SI, Fig. S6). Data demonstrated that the GluSens system had an excellent stability. Though, during the second day an activity of the electrode system dropped to around 80%, but measurements during days 8–10 demonstrated that the relative activity was very close to 100%, thus after 10 days electrodes did not lose any activity. Using the curves from Fig. 4 and three blank measurement values without glucose, we have determined the limit of detection of 0.08 mM glucose and the linear range of the biosensor (1–8 mM).

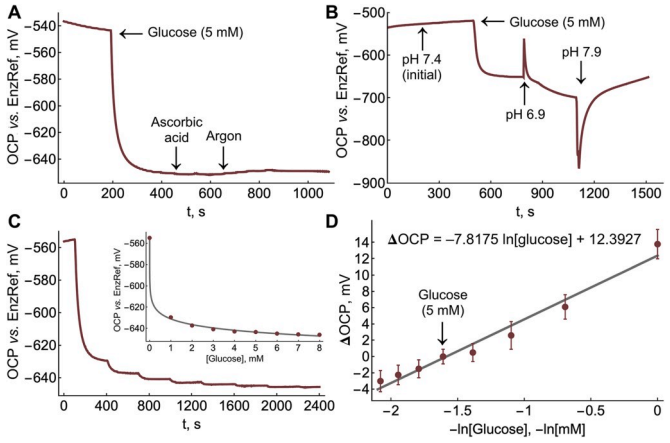

Fig. 4. The electrochemical analysis and calibration curve of GluSens electrode system. **A)** OCP dependence on glucose concentration (5 mM) and possible interference (0.085 mM ascorbic acid and decrease in oxygen concentration). **B)** OCP dependence on pH changes in reaction medium with glucose (5 mM). **C)** Calibration curve of GluSens electrode system, each drop in OCP demonstrates the addition of 1 mM glucose from 0 mM to 8 mM. Inset shows experimental data fit to Nernst equation. **D)** A linearized potentiometric calibration curve depending on glucose concentration (0–8 mM). Blood mimicking WBS pH 7.4. Potential was measured in reference to EnzRef (450 mV *vs.* SCE (694 mV *vs.* SHE)).

In comparison, earlier developed potentiometric glucose biosensors had comparable stabilities, even higher detection limits (up to 0.001 mM) and a wider linear range (0.001 mM–30 mM) (Khun et al., 2012; Usman Ali et al., 2010). However, here we have demonstrated three significant advantages: (1) our biosensor was the 3rd generation – DET was facilitated between enzymes and electrodes, (2) biosensor was capable to differentiate a small change in concentration and could operate in real-time, and, most importantly, (3) metal/salt reference electrode was replaced with fully enzymatic laccase-based reference electrode. Our work could be compared with a recent potentiometric biosensor demonstrated by (Lee et al., 2019), where researchers have demonstrated a potentiometric glucose biosensor based on a DET-capable FAD-glucose dehydrogenase, which had remarkable operation stability of at least 9 days, and a low limit of detection (0.1 mM). The most important advantage of our work compared to the work carried out by Lee et al. is application of laccase-based enzymatic reference electrode and demonstration the system capability to work in human serum.

3.4. Performance of GluSens electrode system for real-time monitoring of glucose

Finally, we have applied the designed GluSens electrode system to measure glucose concentration in real-time. Concentration of glucose was changed in range of 3–8 mM, since those concentrations are typical in physiological conditions. At first, the concentration of glucose was set to 5 mM and after 10 min the GluSens response was –655.0 mV *vs.* EnzRef (Fig. 5). This OCP value was set as a reference potential, according to which ΔOCP was calculated. The concentration of glucose was received using calibration curve:

$$\Delta OCP = \ -7.8175 \ln[glucose] + 12.3927 \quad (3)$$

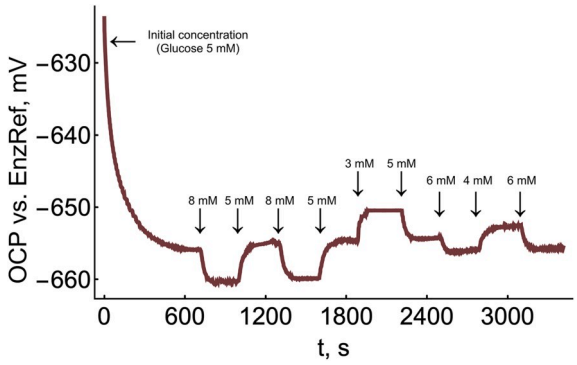

Fig. 5. GluSens electrode system performance for real-time glucose measurement. Glucose concentration was changed in range of 3–8 mM. Blood mimicking WBS pH 7.4. OCP was measured in reference to EnzRef (450 mV *vs.* SCE (694 mV *vs.* SHE)).

Afterwards, the glucose concentration was increased to 8.0 mM. The OCP in less than 2 min dropped to –695.9 mV resulting in ΔOCP of –4.9 mV. When the glucose concentration was changed to 5 mM, the potential value of GluSens electrode system recovered to –655.2 mV giving an ΔOCP of 0.2 mV, which is proportional to 4.76 mM glucose. In the next 45 min. glucose concentration in a cell was changed multiple times. The received data is presented in Table 1 demonstrating that GluSens system is capable of measuring glucose concentration in real-time. Moreover, we would like to note that the electrode system response toward the change in a glucose concentration was very rapid – typical duration for stable potential values were obtained in less than 2 min.

As a proof of concept, we have tested the performance of GluSens electrode system in a commercial human serum sample containing 4.2 mM glucose (SI, Fig. S7). Electrodes were placed in a serum and the potential stabilized at –593.5 mV *vs.* EnzRef. The potential value was higher compared to the measurements conducted in WBS with similar concentration of glucose, most likely due to difference in pH (serum pH – 8.12, while WBS – 7.4). Afterwards, we increased the concentration of glucose by gradually adding 1 mM to the final value of 7.2 mM. The GluSens system responded to the addition of glucose and the potential changes were related to the glucose concentration. The received data was evaluated using calibration curve (equation (3)) (SI, Fig. S7) and presented in Table 1. Data indicate that GluSens system accurately measured glucose concentration in range 4.2–7.2 mM. However, we noticed that the system was less stable compared to operation in WBS – potential values tended to "drift" from the stationary value. We assume this behavior of GluSens system had arisen due to difference in pH and complexity of human serum. Most likely, for prolonged operation in human serum the additional protective membranes would be required.

4. Conclusions

In summary, a real-time glucose monitoring system, containing enzymatic sensor and enzymatic reference electrodes, has been successfully constructed. This was achieved by designing electrode composed of wired glucose dehydrogenase and electrode composed of wired laccase. The electrochemical potential of glucose dehydrogenase electrode was dependent on concentration of glucose, while the potential of laccase electrode was very stable due to ORR. This allowed us to determine glucose concentration in a physiological range (3–8 mM) in real time by measuring the potential difference between two electrodes. Additionally, we have designed protective membrane, which removed the interference of ascorbic acid, urea, ethanol and acetaminophen as well as demonstrated that system is capable of measuring glucose concentration in undiluted human serum. To the best of our knowledge, this is the first fully enzymatic electrode system capable to reference its own potential and avoid usage of metal/salt reference electrode. Our designed enzymatic reference electrode is universal and we envision that it may be applied for other biosensors, thus open possibilities for the new generation of implantable devices for healthcare monitoring.

Table 1
GluSens electrode system performance during real-time glucose measurements in WBS and human serum sample.

Glucose (mM)	GluSens response, ΔOCP (mV)	Found glucose (mM)	Recovery (%)
WBS (pH 7.4)			
3.0	4.50 ± 0.3	2.8 ± 0.1	93 ± 3
4.0	2.20 ± 0.2	3.7 ± 0.1	93 ± 3
5.0	–0.35 ± 0.1	5.1 ± 0.1	102 ± 2
6.0	–1.10 ± 0.15	5.6 ± 0.1	93 ± 2
8.0	–4.90 ± 0.2	9.1 ± 0.2	114 ± 2
Human serum sample (pH 8.12)			
4.2	1.17 ± 0.1	4.2 ± 0.1	100 ± 1
5.2	–0.23 ± 0.2	5.0 ± 0.2	96 ± 5
6.2	–1.43 ± 0.8	5.9 ± 0.6	95 ± 10
7.2	–1.85 ± 1.0	6.2 ± 0.8	86 ± 11

Declaration of competing interest

The authors declare that they have no known competing financial interests or personal relationships that could have appeared to influence the work reported in this paper.

CRediT authorship contribution statement

Lukas Ramašauskas: Investigation, Methodology, Validation, Writing - review & editing, Visualization. **Rolandas Meškys:** Writing - review & editing, Resources. **Dalius Ratautas:** Investigation, Methodology, Conceptualization, Software, Formal analysis, Writing - original draft, Writing - review & editing, Visualization, Supervision.

Acknowledgements

We thank dr. Liucija Marcinkevičienė for the purification of glucose dehydrogenase and laccase enzymes.

Appendix A. Supplementary data

Supplementary data to this article can be found online at https://doi.org/10.1016/j.bios.2020.112338.

Funding

This research did not receive any external funding.

References

Barriet, D., Yam, C.M., Shmakova, O.E., Jamison, A.C., Lee, T.R., 2007. Langmuir 23, 8866–8875. https://doi.org/10.1021/la7007733.
Clark, L.C., Lyons, C., 1962. Ann. N. Y. Acad. Sci. 102, 29–45. https://doi.org/10.1111/j.1749-6632.1962.tb13623.x.
Dagys, M., Laurynėnas, A., Ratautas, D., Kulys, J., Vidžiūnaitė, R., Talaikis, M., Niaura, G., Marcinkevičienė, L., Meškys, R., Shleev, S., 2017. Energy Environ. Sci. 10, 498–502. https://doi.org/10.1039/C6EE02232D.
Das, P., Das, M., Chinnadayyala, S.R., Singha, I.M., Goswami, P., 2016. Biosens. Bioelectron. 79, 386–397. https://doi.org/10.1016/j.bios.2015.12.055.
Falk, M., Blum, Z., Shleev, S., 2012. Electrochim. Acta 82, 191–202. https://doi.org/10.1016/j.electacta.2011.12.133.
Gineitytė, J., Meškys, R., Dagys, M., Ratautas, D., 2019. J. Power Sources 441, 227163. https://doi.org/10.1016/j.jpowsour.2019.227163.
Gutiérrez-Sánchez, C., Jia, W., Beyl, Y., Pita, M., Schuhmann, W., De Lacey, A.L., Stoica, L., 2012. Electrochim. Acta 82, 218–223. https://doi.org/10.1016/j.electacta.2011.12.134.
Häggström, M., 2014. WikiJournal of medicine 1. https://doi.org/10.15347/wjm/2014.008.
Haiss, W., Thanh, N.T.K., Aveyard, J., Fernig, D.G., 2007. Anal. Chem. 79, 4215–4221. https://doi.org/10.1021/ac0702084.

Hashemi, P., Walsh, P.L., Guillot, T.S., Gras-Najjar, J., Takmakov, P., Crews, F.T., Wightman, R.M., 2011. ACS Chem. Neurosci. 2, 658–666. https://doi.org/10.1021/cn2000684.
Khun, K., Ibupoto, Z.H., Lu, J., AlSalhi, M.S., Atif, M., Ansari, A.A., Willander, M., 2012. Sensor. Actuator. B Chem. 173, 698–703. https://doi.org/10.1016/j.snb.2012.07.074.
Kimling, J., Maier, M., Okenve, B., Kotaidis, V., Ballot, H., Plech, A., 2006. J. Phys. Chem. B 110, 15700–15707. https://doi.org/10.1021/jp061667w.
Kizling, M., Dzwonek, M., Więckowska, A., Bilewicz, R., 2018. ChemCatChem 10, 1988–1992. https://doi.org/10.1002/cctc.201800032.
Larpant, N., Pham, A.D., Shafaat, A., Gonzalez-Martinez, J.F., Sotres, J., Sjöholm, J., Laiwattanapaisal, W., Faridbod, F., Ganjali, M.R., Arnebrant, T., Ruzgas, T., 2019. Scientific reports 9. https://doi.org/10.1038/s41598-019-49245-3.
Lee, I., Loew, N., Tsugawa, W., Ikebukuro, K., Sode, K., 2019. Biosens. Bioelectron. 124–125, 216–223. https://doi.org/10.1016/j.bios.2018.09.099.
Pingarrón, J.M., Yáñez-Sedeño, P., González-Cortés, A., 2008. Electrochim. Acta 53, 5848–5866. https://doi.org/10.1016/j.electacta.2008.03.005.
Proksch, E., 2018. J. Dermatol. 45, 1044–1052. https://doi.org/10.1111/1346-8138.14489.
Ramonas, E., Ratautas, D., Dagys, M., Meškys, R., Kulys, J., 2019. Talanta 200, 333–339. https://doi.org/10.1016/j.talanta.2019.03.063.
Ratautas, D., Dagys, M., 2019. Catalysts 10, 9. https://doi.org/10.3390/catal10010009.
Ratautas, D., Marcinkevičienė, L., Meškys, R., Kulys, J., 2015. Electrochim. Acta 174, 940–944. https://doi.org/10.1016/j.electacta.2015.06.063.
Ratautas, D., Ramonas, E., Marcinkevičienė, L., Meškys, R., Kulys, J., 2018. ChemCatChem 10, 971–974. https://doi.org/10.1002/cctc.201701738.
Ratautas, D., Tetianec, L., Marcinkevičienė, L., Meškys, R., Kulys, J., 2017. Biosens. Bioelectron. 98, 215–221. https://doi.org/10.1016/j.bios.2017.06.048.
Scheller, F.W., Schubert, F., Neumann, B., Pfeiffer, D., Hintsche, R., Dransfeld, I., Wollenberger, U., Renneberg, R., Warsinke, A., Johansson, G., Skoog, M., Yang, X., Bogdanovskaya, V., Bückmann, A., Zaitsev, S.Yu, 1991. Biosens. Bioelectron. 6, 245–253. https://doi.org/10.1016/0956-5663(91)80010-U.
Shinwari, M.W., Zhitomirsky, D., Deen, I.A., Selvaganapathy, P.R., Deen, M.J., Landheer, D., 2010. Sensors 10, 1679–1715. https://doi.org/10.3390/s100301679.
Shleev, S., 2017. ChemPlusChem 82, 522–539. https://doi.org/10.1002/cplu.201600536.
Shleev, S., Tkac, J., Christenson, A., Ruzgas, T., Yaropolov, A.I., Whittaker, J.W., Gorton, L., 2005. Biosens. Bioelectron. 20, 2517–2554. https://doi.org/10.1016/j.bios.2004.10.003.
Stoica, L., Ludwig, R., Haltrich, D., Gorton, L., 2006. Anal. Chem. 78, 393–398. https://doi.org/10.1021/ac050327o.
Tetianec, L., Chaleckaja, A., Vidziunaite, R., Kulys, J., Bachmatova, I., Marcinkeviciene, L., Meskys, R., 2014. J. Mol. Catal. B Enzym. 101, 28–34. https://doi.org/10.1016/j.molcatb.2013.12.013.
Thompson, M., Vandenberg, E.T., 1986. Clin. Biochem. 19, 255–261. https://doi.org/10.1016/S0009-9120(86)80037-6.
Usman Ali, S.M., Nur, O., Willander, M., Danielsson, B., 2010. Sensor. Actuator. B Chem. 145, 869–874. https://doi.org/10.1016/j.snb.2009.12.072.
Wang, J., 2008. Chem. Rev. 108, 814–825. https://doi.org/10.1021/cr068123a.
Windmiller, J.R., Wang, J., 2013. Electroanalysis 25, 29–46. https://doi.org/10.1002/elan.201200349.